Understanding the Orientation and Dynamic Motion of Planar Heterocyclic N-Donor Ligands by Exploiting the Symmetry Properties of Mixed-Ligand μ-Oxorhenium(V) Dinuclear Complexes $[ReOCl_2(L)(L')]-O-[ReOCl_2(L)(L')]$: A Combined X-ray Structural and Dynamic NMR Investigation

Enzo Alessio,*,† Ennio Zangrando,† Elisabetta Iengo,† Michela Macchi,† Patricia A. Marzilli,‡ and Luigi G. Marzilli‡

Dipartimento di Scienze Chimiche, Università di Trieste, 34127 Trieste, Italy, and Department of Chemistry, Emory University, Atlanta, Georgia 30322

Received July 20, 1999

Factors influencing the orientation and dynamic motions of planar N-donor heterocyclic ligands (L) are of interest since such features have broad relevance in metallobiochemistry [Marzilli, L. G.; Marzilli, P. A.; Alessio, E. *Pure Appl. Chem.* **1998**, *70*, 961−968]. We found that μ-oxorhenium(V) dinuclear complexes $[ReOCl_2L^sL^t]-O-[ReOCl_2L^sL^t]$ bearing either symmetrical (L = py = pyridine; 3,5-lut = 3,5-lutidine) or lopsided (L = Me_3-Bzm = 1,5,6-trimethylbenzimidazole) *cis* L ligands are particularly useful for studying these factors. NMR data showed that terminal (L^t) and stacked (L^s) ligands were exchanged by ∼180° rotation about the Re−O−Re bond system. Such exchange occurred, however, between degenerate chiral conformers. Here we report a combined X-ray structural and solution NMR investigation of the *AA* + *CC* (*racemic*) and *AC* (*meso*) forms of two mixed-ligand μ-oxorhenium dimers that bear one lopsided and one symmetrical ligand on each Re atom, namely, $Re_2O_3Cl_4(py)_2(Me_3Bzm)_2$ (**1*rac*** and **1*meso***) and $Re_2O_3Cl_4(3,5\text{-lut})_2(Me_3Bzm)_2$ (**2*rac*** and **2*meso***). The presence of two different *cis* L ligands in **1** and **2** breaks the local symmetry at each Re atom, so that, in the racemic dimers, the exchange of terminal and stacked ligands leads to nondegenerate conformers. Overall, NMR data showed that the unsymmetrical dimers **1** and **2** undergo two dynamic processes contemporaneously, namely, 180° rotation about the Re−N(py or 3,5-lut) bond and coupled rotation about the Re−O−Re/Re−N bonds. Both processes reach the slow exchange limit below −80 °C. Rotation of py in **1** occurs faster than that of 3,5-lut in **2**; this difference is attributed to the higher steric demands of 3,5-lut compared to py. For both dimers NMR data provided compelling evidence of the preferred conformers in solution, including ligand orientations. The low-*T* solution structure of **1*meso*** and **2*meso*** is chiral, the same as that found in the solid state for **2*meso***, where the Me_3Bzm on one Re atom is stacked with the 3,5-lut on the other Re atom. The remaining Me_3Bzm and 3,5-lut, one on each Re atom, are both terminal. In solution the coupled Re−O−Re/Re−N rotations interconvert the two halves of each *meso* dimer to yield the same overall stable chiral conformation. For the *racemic* dimers, however, this process does not interconvert one enantiomer into the other, but instead interconverts two rotamers, **R1** and **R2**, each of which is chiral. We found that, in the case of both **1*rac*** and **2*rac***, the conformer with stacking symmetrical ligands (**R1**) is roughly 1 order of magnitude more stable than that with stacking Me_3Bzm ligands (**R2**). Moreover, the solution conformation of **R1** is the same as that found in the solid state of **1*rac***. Solution- and solid-state data indicate that the key interaction favoring the observed conformations is very likely the electrostatic attraction between the δ^+ H2 atoms on the Me_3Bzm ligands and the negative O and Cl groups in the core of the dimers. Finally, for both *meso* and *racemic* dimers we were also able to elucidate the preferred pathways of the coupled dynamic motions and establish that, very likely, the two halves of the dimers swing back and forth by ∼130° through the *anti* eclipsed form.

Introduction

Metal involvement in biology and medicine often entails coordination of planar N-donor heterocyclic ligands (L) such as purines, pyrimidines, imidazoles, etc. In contrast to simple ligands such as pyridine (py), these biological ligands are lopsided and have dipoles directed off the M−N axis and lying in the ligand plane. Such dipoles and the unsymmetrical steric properties of the lopsided ligands influence the dynamic and structural features of the complexes. In most simple metal complexes, these features are difficult to assess since either the orientations of these ligands are restricted by their incorporation into chelate rings or the ligands rotate freely around the metal−nitrogen bond. In only a few cases are the ligand dynamic processes slow enough for the pathways and the ligand orientation to be assessed. As part of a program aimed at investigating factors influencing the orientation and dynamic motions of such ligands, we have been investigating some of the rare examples in which such assessments can be made. In some cases the metals are abiological.

A particularly informative type of complex has the general formula $Re_2O_3Cl_4(L)_4$. Such oxorhenium(V) dinuclear complexes (referred to hereafter as dimers) have been known for a

* To whom correspondence should be addressed. Phone: +39 040 6763961. Fax: +39 040 6763903. Email: alessi@univ.trieste.it.
† Università di Trieste.
‡ Emory University.

10.1021/ic990858t CCC: $19.00
Published on Web 01/04/2000

long time;[1] they contain the almost linear O═Re−O−Re═O moiety with the μ-oxo bridge, and each Re atom bears two *cis* chlorides and two ligands.[2] In this study we examine the *AA* + *CC* (*racemic*) and *AC* (*meso*) forms of compounds containing two different ligands, namely, $Re_2O_3Cl_4(py)_2(Me_3Bzm)_2$ (**1**; Me_3-Bzm = 1,5,6-trimethylbenzimidazole) and $Re_2O_3Cl_4(3,5\text{-lut})_2(Me_3Bzm)_2$ (**2**; 3,5-lut = 3,5-lutidine). Structural studies by us and by others on $Re_2O_3Cl_4(Me_3Bzm)_4$ (**3**),[3,4] $Re_2O_3Cl_4(pyz)_4$ (pyz = pyrazine),[5] $Re_2O_3Cl_4(py)_4$ (**4**),[6] and $Re_2O_3Cl_4(3,5\text{-}Me_2pzH)_4$ (pzH = pyrazole)[7] have established a common feature: in the solid-state conformation, one L ligand on each Re atom is stacked with the corresponding L on the other Re (L^s for "stacked"), while the other is designated as L^t for "terminal". We introduced the use of lopsided ligands in these systems because the structure of $Re_2O_3Cl_4(py)_4$ in the solid state led to the hypothesis that there might be restricted rotation in solution,[6] as we indeed demonstrated.[3,4]

We developed a very informative strategy of comparing the stereochemistry and dynamic behavior of analogous metal complexes with symmetrical N-donor ligands and with lopsided ligands of interest in biological systems.[8] This strategy has now been adopted by others.[9] Using 2D exchange nuclear Overhauser effect spectroscopy (NOESY/EXSY), we investigated the solution conformations of two oxorhenium(V) dimers, one with the symmetrical ligand 3,5-lutidine, $Re_2O_3Cl_4(3,5\text{-lut})_4$ (**5**), and the other with the lopsided ligand 1,5,6-trimethylbenzimidazole, $Re_2O_3Cl_4(Me_3Bzm)_4$ (**3**).[4] We found that both $Re_2O_3Cl_4(3,5\text{-lut})_4$ and $Re_2O_3Cl_4(Me_3Bzm)_4$ have a complicated dynamic behavior in solution that involves rotation about the Re−O−Re bond system and also about the Re−N bonds. These motions exchange the stacking ligands with the terminal ones in a pairwise fashion. The local symmetry on each Re atom required that exchange occurred between two equivalent conformations (topomers) with opposite chirality.

Two lopsided ligands attached to the same metal atom in *cis* positions can be related in a head-to-head (HH) or head-to-tail (HT) orientation. In the present case, we define the H2 of Me_3-Bzm (Chart 1) as the tip of the head. The stacked Me_3Bzm ligands of the $Re_2O_3Cl_4(Me_3Bzm)_4$ dimer can also have an HH or an HT orientation, although in this case the ligands are on different metal atoms.

We have recently developed a new synthetic approach that allowed us to prepare unprecedented oxorhenium(V) dimers having two different *cis* L ligands on each Re atom.[10] When the two N-donor ligands are different from each other, the mononuclear hydroxo intermediate used in our new method is chiral (Scheme 1). Therefore, a racemic mixture of *AA* or *CC* enantiomeric dimers will form from the combination of two monomers with the same chirality, while an *AC* (*meso*) dimer will result from the combination of two monomers with opposite chirality.

These dimers, by virtue of lacking local symmetry on each Re atom, have now provided new information on factors influencing lopsided ligand orientation. In this paper we report a combined X-ray structural and solution NMR investigation of such mixed-ligand dimers. This new information benefits from past related studies in which dimers bearing only a single type of L ligand, either lopsided or symmetrical, were so investigated.[3,4]

Chart 1. Numbering Scheme and the Interligand NOE Connectivity Path for the Me_3Bzm Ligand[a]

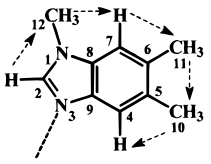

[a] The carbons are designated "B" (for benzimidazole) in the references to NMR results in the text.

Scheme 1. Proposed Reaction Pathway from *mer*-$ReOCl_3(OPPh_3)(L_1)$ to *AA* + *CC* (*racemic*) and *AC* (*meso*) Mixed-Ligand Dimeric Species $[ReOCl_2(L_1)(L_2)]$−O−$[ReOCl_2(L_1)(L_2)]$, through the Unstable Chiral *A*/*C* Intermediate $[ReO(OH)Cl_2(L_1)(L_2)]$[a]

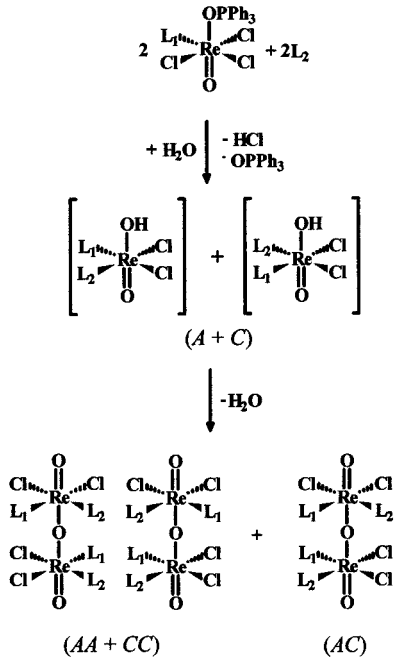

[a] The eclipsed forms of the dimers are shown.

Experimental Section

Reagents. Analytical grade solvents were used without further purification. All reagents, including CD_2Cl_2 and $CDCl_3$, were from Aldrich.

Starting Materials. $ReOCl_3(OPPh_3)(Me_3Bzm)$ was prepared by known methods.[10]

***AA* + *CC* $Re_2O_3Cl_4(py)_2(Me_3Bzm)_2$ (1*rac*).** Pyridine (32 μL, 0.4 mmol) dissolved in 10 mL of acetone was added dropwise to a magnetically stirred suspension of *mer*-$ReOCl_3(OPPh_3)(Me_3Bzm)$ (300 mg, 0.4 mmol) in 10 mL of acetone. The emerald green solution

(1) Johnson, N. P.; Taha, F. I. M.; Wilkinson, G. *J. Chem. Soc.* **1964**, 2614−2616.
(2) The structural characterizations of two all-*trans* dimers, $Re_2O_3Cl_4(1\text{-Meim})_4$ (1-Meim = 1-methylimidazole) and $Re_2O_3Cl_4(py)_4$, have been reported: ($Re_2O_3Cl_4(1\text{-Meim})_4$) Pearson, C.; Beauchamp, A. L. *Acta Crystallogr.* **1994**, *C50*, 42−44. ($Re_2O_3Cl_4(py)_4$) Fortin, S.; Beauchamp, A. L. *Inorg. Chim. Acta* **1998**, *279*, 159−164.
(3) Marzilli, L. G.; Iwamoto, M.; Alessio, E.; Hansen, L.; Calligaris, M. *J. Am. Chem. Soc.* **1994**, *116*, 815−816.
(4) Alessio, E.; Hansen, L.; Iwamoto, M.; Marzilli, L. G. *J. Am. Chem. Soc.* **1996**, *118*, 7593−7600.
(5) Alessio, E.; Zangrando, E.; Mestroni, S. Unpublished work.
(6) Lock, C. J. L.; Turner, G. *Can. J. Chem.* **1978**, *56*, 179−188.
(7) Backes-Dahmann, G.; Enemark, J. H. *Inorg. Chem.* **1987**, *26*, 3960−3962.
(8) (a) Iwamoto, M.; Alessio, E.; Marzili, L. G. *Inorg. Chem.* **1996**, *35*, 2384−2389. (b) Alessio, E.; Calligaris, M.; Iwamoto, M.; Marzilli, L. G. *Inorg. Chem.* **1996**, *35*, 2538−2545. (c) Alessio, E.; Zangrando, E.; Roppa, R.; Marzilli, L. G. *Inorg. Chem.* **1998**, *37*, 2458−2463.
(9) Velders, A. H.; Hotze, A. C. G.; Haasnoot, J. G.; Reedijk, J. *Inorg. Chem.* **1999**, *38*, 2762−2763.
(10) Hansen, L.; Alessio, E.; Iwamoto, M.; Marzilli, P. A.; Marzilli, L. G. *Inorg. Chim. Acta* **1995**, *240*, 413−417.

obtained after 30 min was stored at 4 °C after removal (filtration over fine paper) of some white precipitate. Deep green crystals suitable for X-ray investigation (hexagonal plates) formed overnight and were removed by filtration, washed with water, cold acetone, and diethyl ether and vacuum-dried at 25 °C (yield 40 mg, 20%). Anal. Calcd for $C_{30}H_{34}N_6Cl_4O_3Re_2$ (MW = 1040.84): C, 34.6; H, 3.29; N, 8.07. Found: C, 35.1; H, 3.41; N, 7.95. Selected IR absorption bands: KBr, $\nu_{Re=O}$ 969 cm^{-1} (m), $\nu_{Re-O-Re}$ 687 cm^{-1} (vs). UV/vis spectrum (λ_{max}, nm (ϵ, M^{-1} cm^{-1}) (in $CHCl_3$ solution): 677 (350) br. Concentration of the mother liquor yielded only a small amount of *mer*-$ReOCl_3(OPPh_3)$(py). When the reaction was repeated in a smaller volume of acetone, i.e., under the same conditions used for **2** (see below), an abundant emerald green precipitate formed within 1 h after the reagents were mixed. The product was collected by filtration, washed with water, cold acetone, and diethyl ether, and vacuum-dried at 25 °C (yield 115 mg, 55%). ^{1}H NMR analysis showed it to be a mixture of "racemic" and "meso" dimer $Re_2O_3Cl_4(py)_2(Me_3Bzm)_2$ (**1***rac* and **1***meso*) in a ca. 1:0.5 ratio.

***AA*+*CC* $Re_2O_3Cl_4$(3,5-lut)$_2(Me_3Bzm)_2$ (2*rac*).** 3,5-lut (60 μL, 0.52 mmol) was added to a magnetically stirred suspension of *mer*-$ReOCl_3(OPPh_3)(Me_3Bzm)$ (300 mg, 0.4 mmol) in 7 mL of acetone. The mixture turned immediately from light to emerald green, and a precipitate of the same color rapidly formed and gradually replaced the starting material. After 90 min the product was collected by filtration, washed with water, cold acetone, and diethyl ether, and vacuum-dried at 25 °C (yield 55 mg, 25%). Anal. Calcd for $C_{34}H_{42}N_6Cl_4O_3Re_2$ (MW = 1096.97): C, 37.2; H, 3.87; N, 7.51. Found: C, 36.9; H, 3.86; N, 7.47. Selected IR absorption bands: KBr, $\nu_{Re=O}$ 970 cm^{-1} (m), $\nu_{Re-O-Re}$ 688 cm^{-1} (vs). UV/vis spectra (λ_{max}, nm (ϵ, M^{-1} cm^{-1}) (in $CHCl_3$ solution): 680 (360) br.

AC* $Re_2O_3Cl_4$(3,5-lut)$_2(Me_3Bzm)_2$ (2*meso*).** The mother liquor of the synthesis of **2rac* was concentrated to ~3 mL by rotary evaporation (without heating) and stored at 4 °C after addition of a few drops of diethyl ether. Emerald green plates formed overnight and were collected by filtration, washed with water, cold acetone, and diethyl ether, and vacuum-dried at 25 °C (yield 20 mg, 9%). Anal. Calcd for $C_{34}H_{42}N_6Cl_4O_3Re_2 \cdot {}^1/_2(CH_3)_2CO$ (MW = 1126.01): C, 37.8; H, 4.03; N, 7.46. Found: C, 37.6; H, 3.98; N, 7.42. ^{1}H NMR and IR spectra showed that when the product precipitated as a microcrystalline aggregate, also after being dried at 100 °C for 10 h, it contained variable amounts of acetone and diethyl ether. Selected IR absorption bands: KBr, $\nu_{Re=O}$ 968 cm^{-1} (m), $\nu_{Re-O-Re}$ 690 cm^{-1} (vs). UV/vis spectrum (λ_{max}, nm (ϵ, M^{-1} cm^{-1}) (in $CHCl_3$ solution): 686 (430) br.

NMR Spectroscopy. NMR spectra, recorded on a JEOL EX400 spectrometer, were referenced to TMS. ^{1}H 1D data were collected typically with a 6000 Hz window, a 30° pulse width, and 32K data points. 2D parameters include a 512 × 1024 matrix, 16 scans per t_1 increment preceded by 2 dummy scans, a spectral window of 3700 Hz, a pulse delay of 2.36 s, a mixing time of 500 ms, zero filling of the second dimension to 1024 data points prior to Fourier transformation, and a square sine bell function with no phase shift applied in both dimensions.

X-ray Crystallography. Crystal data and data collection and refinement parameters for compounds **1***rac* and **2***meso* are summarized in Table 1. Unit cell parameters for **1***rac* were obtained by least-squares treatment of 25 reflections in the θ range of 11−18°. A total of 5630 data were collected at room temperature on a hexagonal prism-shaped crystal (0.30 × 0.30 × 0.07 mm) using the $\omega/2\theta$ scan technique on a CAD4 Enraf-Nonius diffractometer, equipped with a graphite monochromator with Mo Kα radiation (λ = 0.710 73 Å, $2\theta_{max}$ = 60°). Intensities of three standard reflections measured during data collection did not show any significant decay. The reflections were corrected for Lorentz-polarization effects and used for structure determination. An absorption correction, based on an empirical Ψ-scan, was applied (maximum and minimum transmission factors (%) 99.9 and 83.7). Data collection for **2***meso* (small green plate with dimensions 0.06 × 0.06 × 0.02 mm) was carried out at the X-ray diffraction beamline of the Elettra Synchrotron, Trieste (Italy), on a 30 cm MAR imaging plate (λ = 0.800 Å by using a double-crystal Si(111) monochromator). A total of 23 frames were collected at 100 K over a quarter of the reciprocal space with rotation of 4° about φ with a fixed dose of radiation, the detector being positioned at a distance of 100 mm from the crystal. A total of 21 265 reflections were collected, 7028 of which were unique (R_{int} = 0.063). Data reduction and cell refinement were carried out using the program DENZO.[11] Reflections partially measured on the previous and following frames were used to scale these frames to each other, a procedure that partially eliminated absorption effects while also taking into account any crystal decay. Both the structures were solved by the standard Patterson method and Fourier syntheses.[12] A difference Fourier map of **2***meso* revealed the presence of a disordered acetone molecule (occupancy factor of 0.5 based on the electron density peaks). Final cycles of refinement (SHELXL-97),[13] with the contribution of hydrogen atoms placed at geometrically calculated positions (except those of the acetone molecule in **2***meso*), converged to the *R* factors reported in Table 1.

Table 1. Crystallographic Data for *rac*-$Re_2O_3Cl_4(py)_2(Me_3Bzm)_2$ (**1***rac*) and *meso*-$Re_2O_3Cl_4$(3,5-lut)$_2(Me_3Bzm)_2$ (**2***meso*)

	1*rac*	**2***meso*
empirical formula	$C_{30}H_{34}N_6Cl_4O_3Re_2$	$C_{34}H_{42}N_6Cl_4O_3Re_2 \cdot 0.5(CH_3)_2CO$
fw	1040.83	1126.01
T, K	293(2)	100(2)
cryst syst	orthorhombic	orthorhombic
space group	*Pbcn* (No. 60)	*Pbca* (No. 61)
a, Å	14.384(4)	17.113(3)
b, Å	10.265(5)	20.744(4)
c, Å	23.571(5)	23.302(6)
V, Å^3	3480(2)	8272(3)
Z	4	8
λ, Å	0.710 73	0.800 00
$\rho_{(calcd)}$, g cm^{-3}	1.986	1.808
μ, mm^{-1}	7.297	6.149
R1[a]	0.0628	0.0522
wR2[a]	0.0831[b]	0.1354[c]

[a] $R1 = \sum||F_o| - |F_c||/\sum|F_o|$, $wR2 = [\sum w(F_o^2 - F_c^2)^2/\sum w(F_o^2)^2]^{1/2}$. [b] $w = 1/[\sigma^2(F_o^2) + (0.0218P)^2]$. [c] $1/[\sigma^2(F_o^2) + (0.0616P)^2 + 109.49P]$, where $P = [\max(F_o^2,0) + 2F_c^2]/3$.

Results

Previously we found[3,4] that treatment of $ReOCl_3(Me_2S)(OPPh_3)$[14,15] with an excess of L (L = Me_3Bzm, 3,5-lut, or py) in wet acetone or benzene leads to replacement of both the Me_2S and $OPPh_3$, affording $Re_2O_3Cl_4L_4$ dimers. Later,[10] we found that this dimerization can also be performed in a stepwise manner, thus opening a route to the formation of mixed-L dimeric species. Treatment of $ReOCl_3(Me_2S)(OPPh_3)$ with 1 equiv of L led to substitution of Me_2S only and formation of $ReOCl_3(OPPh_3)$(L). The crystal structure of the Me_3Bzm derivative *mer*-$ReOCl_3(OPPh_3)(Me_3Bzm)$ established the geometry.[10] Reaction of the latter with 1 equiv of py or 3,5-lut in acetone having adventitious water led to the formation of the mixed-ligand dimeric species $Re_2O_3Cl_4(py)_2(Me_3Bzm)_2$ (**1**) and $Re_2O_3Cl_4$(3,5-lut)$_2(Me_3Bzm)_2$ (**2**), respectively.[10] Dimers **1** and **2** can be thought of as deriving from the condensation of two units of $ReO(OH)Cl_2(py)(Me_3Bzm)$ and $ReO(OH)Cl_2$(3,5-lut)(Me_3Bzm), respectively (Scheme 1). Such hydroxo intermediates have also been postulated in the formation of $Re_2O_3Cl_4L_4$ dimers.[1] However, in our case the intermediate is chiral, and a statistical mixture (25:25:50) of *AA* and *CC* (*enantiomeric*) and *AC* (*meso*) dimers might be expected to form.

(11) Otwinowsky, Z.; Minor, W. *Methods Enzymol.* **1997**, *276*, 307−326.
(12) Sheldrick, G. M. *Acta Crystallogr., Sect. A* **1990**, *A46*, 467−473.
(13) Sheldrick, G. M. SHELXL-97, Program for crystal structure refinement, University of Göttingen, Germany, 1997.
(14) Grove, D. E.; Wilkinson, G. *J. Chem. Soc. A* **1966**, 1224−1230.
(15) Bryan, J. C.; Stenkamp, R. E.; Tulip, T. H.; Mayer, J. M. *Inorg. Chem.* **1987**, *26*, 2283−2288.

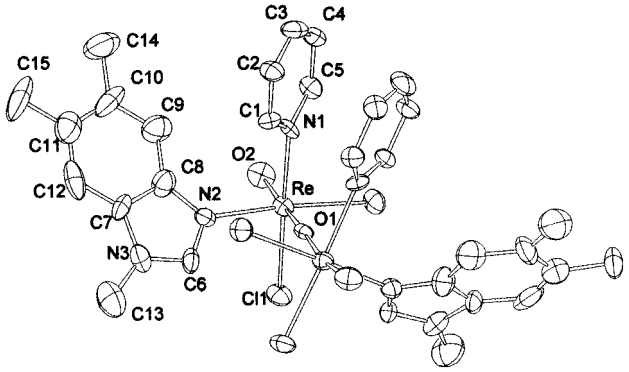

Figure 1. ORTEP drawing of the complex *rac*-$Re_2O_3Cl_4(py)_2(Me_3Bzm)_2$ (**1*rac***) with thermal ellipsoids at 40% probability. Only atoms of the crystallogaphically independent part are labeled.

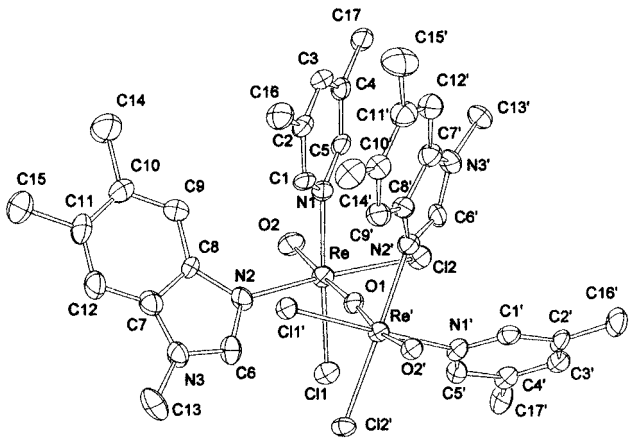

Figure 2. ORTEP drawing of the complex *meso*-$Re_2O_3Cl_4(lut)_2(Me_3Bzm)_2$ (**2*meso***) and atom labeling scheme (thermal ellipsoids at 40% probability).

NMR and X-ray structural studies (see below) proved that the poorly soluble emerald green precipitates formed after $ReOCl_3(OPPh_3)(Me_3Bzm)$ was mixed with py and 3,5-lut are racemic mixtures of *AA* + *CC* enantiomeric dimers, *rac*-$Re_2O_3Cl_4(py)_2(Me_3Bzm)_2$ (**1*rac***) or *rac*-$Re_2O_3Cl_4(3,5\text{-lut})_2(Me_3Bzm)_2$ (**2*rac***), respectively. A second green precipitate was isolated in pure form from the concentrated mother liquor of **2*rac***; its elemental analysis, UV/vis and IR spectra are almost identical to those of the first precipitate, but its ^1H NMR spectrum is remarkably different from that of **2*rac***. This product was shown by NMR and X-ray structural investigation (see below) to be the *AC* (*meso*) form of the same dimer, *meso*-$Re_2O_3Cl_4(3,5\text{-lut})_2(Me_3Bzm)_2$ (**2*meso***). Concentration of the mother liquor of **1*rac*** led to the isolation of only some *mer*-$ReOCl_3(OPPh_3)(py)$, indicating that substitution of Me_3Bzm rather than of $OPPh_3$ had also occurred in the precursor. The corresponding pyridine dimers could be obtained only in a ca. 1 (**1*rac***):0.5 (**1*meso***) mixture by performing the synthesis in a more concentrated solution. We also found that cooling a solution of **2*meso*** in the minimum volume of acetone after it had been heated at reflux for 30 min yielded a green precipitate. This was identified by NMR as the less soluble **2*rac*** mixture.

Structural Studies. The *racemic* form of $Re_2O_3Cl_4(py)_2(Me_3Bzm)_2$ (**1*rac***) and the *meso* form of $Re_2O_3Cl_4(3,5\text{-lut})_2(Me_3Bzm)_2$ (**2*meso***) crystallyzed. Both structures (Figures 1 and 2 and Table 2) contain a nearly linear O═Re−O−Re═O group; in **1*rac*** the μ-oxo ligand is located on a crystallographic 2-fold axis relating the two halves of the dimer. In both dimers the coordination about Re is pseudooctahedral. The Re−N bond lengths, ranging from 2.100(9) to 2.164(9) Å (Table 2), are similar within experimental error, and no relationship to the basicity of the N ligands is apparent. The Re−Cl, the Re−O(bridge), and Re−O(terminal) distances of **1*rac*** are comparable within their esd's with those detected in **2*meso***, and also with those found in dimers **3**[4] and **4**.[6] The metals in both the structures are slightly displaced (up to 0.12 Å for Re′ in **2*meso***) from the equatorial N_2Cl_2 mean plane (maximum deviation being ±0.015 Å) toward the terminal oxo ligand. For all the Me_3Bzm ligands, the Re−N(2)−C(6) and Re−N(2)−C(8) bond angles are close to about 122° and 131°, respectively. Such an unsymmetrical coordination disposition of Me_3Bzm is a well-documented feature of Ru(II)[8] and Co(III) complexes.[16] Moreover the N ligands are rotated about the respective Re−N bond by ∼40−50° away from coplanarity with this N_2Cl_2 plane. The dihedral angles formed by the ligand mean planes are 53.5(3)° (py/Me_3Bzm in **1*rac***) and 55.9(3)° and 58.3(3)° (3,5-lut/Me_3Bzm in **2*meso***) (Table 2).

Rotation of the two halves of the dimer about the Re−Re′ vector away from an eclipsed conformation allows stacking of the pyridines in **1*rac*** and a 3,5-lut/Me_3Bzm pair in **2*meso***. A perspective view of the intramolecular stacking interaction is shown in Figure 3. The shortest interplanar distance between the facing bases is 3.14 Å (py^s in **1*rac***) and 3.21 Å (lut^s−Me_3Bzm^s in **2*meso***). If the intermetallic Re−Re′ vector is treated

Table 2. Selected Coordination Bond Lengths (Å) and Angles (deg) and Some Relevant Geometric Parameters for Dimers *rac*-$Re_2O_3Cl_4(py)_2(Me_3Bzm)_2$ (**1*rac***) and *meso*-$Re_2O_3Cl_4(3,5\text{-lut})_2(Me_3Bzm)_2$ (**2*meso***)

	1*rac*	**2*meso***[a]	
Re−O(2)	1.671(7)	1.669(7)	1.683(7)
Re−O(1)	1.915(1)	1.899(7)	1.923(7)
Re−N(2)	2.120(8)	2.100(9)	2.131(8)
Re−N(1)	2.156(7)	2.164(9)	2.135(8)
Re−Cl(1)	2.368(3)	2.376(3)	2.376(2)
Re−Cl(2)	2.387(3)	2.399(3)	2.366(2)
O(2)−Re−O(1)	170.0(3)	170.2(3)	168.6(3)
O(2)−Re−N(2)	90.9(3)	91.0(4)	88.6(3)
O(1)−Re−N(2)	85.0(2)	85.6(3)	82.4(3)
O(2)−Re−N(1)	87.6(3)	85.7(3)	88.7(3)
O(1)−Re−N(1)	83.5(3)	85.2(3)	83.9(3)
N(2)−Re−N(1)	91.9(3)	92.6(3)	87.4(3)
O(2)−Re−Cl(1)	97.5(3)	98.1(3)	97.7(2)
O(1)−Re−Cl(1)	91.4(3)	91.0(2)	89.6(2)
N(2)−Re−Cl(1)	87.7(2)	87.7(3)	91.8(2)
N(1)−Re−Cl(1)	174.8(2)	176.2(2)	173.5(2)
O(2)−Re−Cl(2)	95.7(2)	94.4(3)	97.5(2)
O(1)−Re−Cl(2)	88.82(8)	89.2(2)	91.3(2)
N(2)−Re−Cl(2)	173.2(2)	174.5(2)	173.6(3)
N(1)−Re−Cl(2)	90.3(2)	88.8(2)	90.7(2)
Cl(1)−Re−Cl(2)	89.65(9)	90.60(9)	89.45(9)
Re−O(1)−Re′	176.9(5)	175.1(4)	
Re−N2−C6	121.7(7)	123.3(7)	123.3(8)
Re−N2−C8	131.6(8)	132.7(7)	129.1(8)
N^s−Re···Re′−N^s	−23.8(4)	−24.6(3)	
N^t−Re···Re′−N^t	151.4(4)	154.5(3)	
interbase angle[b]	53.5(3)	55.9(3)	58.3(3)
py[c]/N_2Cl_2	45.8(2)	44.7(3)	51.4(3)
Me_3Bzm/N_2Cl_2	42.6(2)	39.8(3)	42.2(2)

[a] The second column of **2*meso*** refers to the primed atoms of Figure 2. [b] Angle between bases at the same metal. [c] 3,5-lut in **2*meso***.

(16) (a) Yohannes, P. G.; Bresciani-Pahor, N.; Randaccio, L.; Zangrando, E.; Marzilli, L. G. *Inorg. Chem.* **1988**, *27*, 4738−4744. (b) Parker, W. O., Jr.; Zangrando, E.; Bresciani-Pahor, N.; Marzilli, P. A.; Randaccio, L.; Marzilli, L. G. *Ibid.* **1988**, *27*, 2170. (c) Charland, J.-P.; Attia, W. M.; Randaccio, L.; Marzilli, L. G. *Organometallics* **1990**, *9*, 1367−1375. (d) Charland, J.-P.; Zangrando, E.; Bresciani-Pahor, N.; Randaccio, L.; Marzilli, L. G. *Inorg. Chem.* **1993**, *32*, 4256−4267.

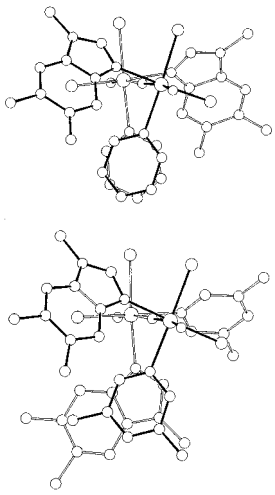

Figure 3. Side view of the complexes *rac*-$Re_2O_3Cl_4(py)_2(Me_3Bzm)_2$ (**1*rac***) (top) and *meso*-$Re_2O_3Cl_4(lut)_2(Me_3Bzm)_2$ (**2*meso***) (bottom) showing the base stacking. The full bonds pertain to the front Re atom.

as a bond, the $N^s-Re\cdots Re'-N^s$ torsion angle is 23.8(4)° in **1*rac*** and 24.6(3)° in **2*meso***, respectively; these are comparable to values of 28° and 23° found in $Re_2O_3Cl_4(Me_3Bzm)_4$ (**3**)[4] and $Re_2O_3Cl_4(py)_4$ (**4**),[6] respectively. On the other hand, the two terminal bases are far apart and the $N^t-Re\cdots Re'-N^t$ "torsion angle" is 151.4(4)° in **1*rac***, the corresponding figure in **2*meso*** being 154.5(3)°. These values are comparable to 152.1° and 155.1° found in **3** and **4**, respectively.[4,6]

The overall molecular conformation with pairs of stacking and terminal bases of the present complexes is very close to that found for $Re_2O_3Cl_4(Me_3Bzm)_4$ (**3**)[4] and $Re_2O_3Cl_4(py)_4$ (**4**).[6] In particular, the overall conformation of **1*rac*** resembles that of **3**, with the pyridines replacing the two stacking Me_3Bzm ligands (Me_3Bzm^s), while that of **2*meso*** can be similarly derived from that of **3** by replacing the Me_3Bzm^s on one Re atom and the Me_3Bzm^t on the other with 3,5-lut ligands. The conformations of **1*rac*** and **2*meso*** in the solid state are both chiral; the dimers crystallize in centrosymmetric space groups, and therefore the chiral rotamers exist as enantiomeric pairs in the unit cells.

The staggered conformation allows two bases to stack, even if both are canted with respect to the N_2Cl_2 plane. In a *syn* eclipsed conformation, two pairs of bases would be aligned between the two halves of the dimer; however, because they are canted, the bases could not stack. Additionally, there would be electrostatic repulsions between the chloro ligands. There are other possible conformations with the overall staggered structure. For example, the lopsided ligand could point in the direction opposite to that found in the crystals; in the case of **1*rac***, the lopsided Me_3Bzm ligands could be stacked. However, the key type of interaction that favors the observed conformations is very likely the attractive interaction between the positive head of terminal Me_3Bzm ligands, defined by the H2 end, and the negative, central core of the dimer, i.e., the nearly eclipsed Cl groups *trans* to the py ligands in **1*rac*** (two electrostatic attractions) and *trans* to $lut^s-MeBzm^s$ in **2*meso***. This interaction dictates the Me_3Bzm orientation.

NMR Spectroscopy. At 20 °C both $Re_2O_3Cl_4(py)_2(Me_3Bzm)_2$ (**1*rac*** and **1*meso***) and $Re_2O_3Cl_4(3,5\text{-lut})_2(Me_3Bzm)_2$ (**2*rac*** and **2*meso***) have only one set of resonances, with the chemically, but not magnetically, equivalent protons (α- and β-H in **1** and α-H and β-CH_3 in **2**) having a single resonance with double intensity compared to the aromatic and methyl signals of Me_3-Bzm. Pyridine resonances were assigned by means of COSY spectra; assignments of Me_3Bzm and 3,5-lut signals were made by means of NOESY spectra (see below). As in previous papers, in discussing the Me_3Bzm parameters, we use the numbers in Chart 1 and refer to carbons as B2, etc. The Me_3Bzm shifts are remarkably similar for dimers **1*rac*** and **2*rac***; this is true as well for dimers **1*meso*** and **2*meso*** (Supporting Information). On the contrary, the Me_3Bzm resonances of both *racemic* dimers are remarkably different from those of the corresponding *meso* forms. These results indicate that the members of each pair of dimers have very similar conformations in solution.

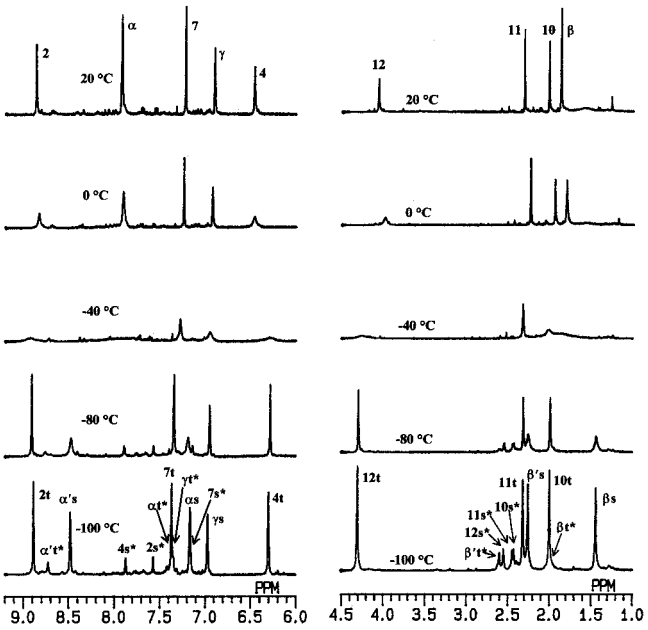

Figure 4. ^1H NMR spectra of *rac*-$Re_2O_3Cl_4(3,5\text{-lut})_2(Me_3Bzm)_2$ (**2*rac***) in CD_2Cl_2 at various temperatures in the downfield (A, left) and upfield (B, right) regions. Signal assignments for the stacked (s) and terminal (t) ligands are indicated. Signals of **R2** protons are marked with an asterisk.

The small number of NMR resonances observed for **1** and **2** at ambient *T* suggests that both dimers, like the similar C_2-symmetric $Re_2O_3Cl_4(Me_3Bzm)_4$ and $Re_2O_3Cl_4(3,5\text{-lut})_4$ dimers,[3,4] are fluxional molecules. At 20 °C all py resonances of **1*rac*** and **1*meso*** are sharp, but several 3,5-lut signals of **2*rac*** and **2*meso*** are slightly broad. *Racemic* and *meso* dimers will be addressed separately.

AA* + *CC* Dimers 1*rac* and 2*rac*.** Below 0 °C, all peaks of *rac*-$Re_2O_3Cl_4(3,5\text{-lut})_2(Me_3Bzm)_2$ (**2*rac) are broad and nearly undetectable at ca. −50 °C. However, at very low *T* (−80 °C) the signals sharpen and two sets of resonances with a ca. 7:1 intensity ratio emerge (Figure 4); in the major set, six aromatic and five methyl singlets are observed. The *T* dependence of the spectrum of *rac*-$Re_2O_3Cl_4(py)_2(Me_3Bzm)_2$ is qualitatively similar to that of **2*rac*** (intensity ratio between the two sets ca. 10:1 at −100 °C), even though at −100 °C some pyridine resonances are still rather broad. At −100 °C the Me_3Bzm resonances in both sets of signals of **1*rac*** are very similar to those found in the corresponding sets of **2*rac***. Therefore, it is clear that **1*rac*** and **2*rac*** undergo similar dynamic processes.

AC* Dimers 1*meso* and 2*meso*.** As for **2*rac, all the signals of *meso*-$Re_2O_3Cl_4(3,5\text{-lut})_2(Me_3Bzm)_2$ (**2*meso***) broaden considerably below 0 °C and are nearly undetectable at ca. −60 °C. At −80 °C two sets of signals of equal abundance appear and become relatively sharp at −100 °C, totaling 12 aromatic and 10 methyl resolved singlets (Figure 5).

The *T* dependence of the ^1H NMR spectrum of *meso*-$Re_2O_3Cl_4(py)_2(Me_3Bzm)_2$ (**1*meso***) is qualitatively similar to that of

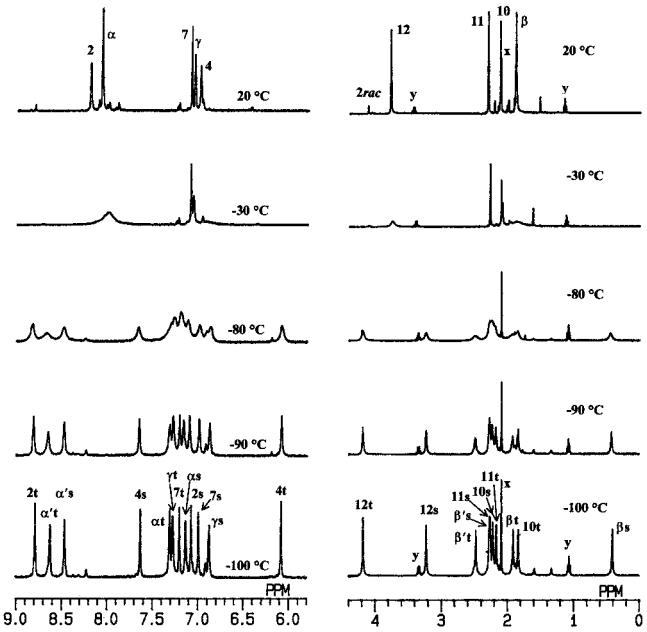

Figure 5. ^{1}H NMR spectra of *meso*-$Re_2O_3Cl_4(3,5\text{-lut})_2(Me_3Bzm)_2$ (**2*meso***) in CD_2Cl_2 at various temperatures in the downfield (A, left) and upfield (B, right) regions. Signal assignments for the stacked (s) and terminal (t) ligands are indicated. Traces of acetone and diethyl ether are marked with x and y, respectively.

2*meso*. However, the pyridine resonances of both sets, and of one in particular, are still broad at the lowest *T* reached in CD_2Cl_2 (−110 °C), making COSY connections within each set almost undetectable. Moreover, **1*meso*** was always obtained in an approximately equimolar mixture with **1*rac***, and several resonances of the two isomers overlap in the low-*T* spectrum, further complicating the spectral assignment of **1*meso***.

Discussion

Dynamic Processes. In discussing the solution structure and dynamic behavior of **1** and **2**, we first review our results on the C_2-symmetric dimers $Re_2O_3Cl_4(Me_3Bzm)_4$ (**3**) and $Re_2O_3Cl_4(3,5\text{-lut})_4$ (**5**).[3,4] Two types of dynamic processes influence the NMR spectrum of such dimers: (1) rotation about the Re−O−Re bonds and (2) rotation about the Re−N bonds; combinations of the two processes can occur.

A ∼180° rotation about the Re−O−Re bond system (either one ∼180° rotation about one Re−O bond or one ∼90° rotation about each Re−O bond) exchanges the stacking ligands with the terminal ones in a pairwise fashion and, when it is fast on the NMR time scale, involves the averaging of their resonances. We had shown that, in C_2-symmetric $Re_2O_3Cl_4(L)_4$ dimers, such as **3** and **5**, this overall dynamic process inverts the chirality of the dimer, and since the L ligand planes lie between the adjacent bonds and not along them, at some point during the inversion each of the L ligands *must* also rotate by a net ∼90° about the Re−N bond. The two motions, ∼180° Re−O−Re rotation and ∼90° Re−N rotation, are coupled.[4]

Even though several types of motion about the metal−N bonds can be envisioned, we found only 180° rotations for 3,5-lut in **5**.[4] We found a similar result for *cis,cis,cis*-$RuCl_2(Me_2SO)_2(L)(L')$ complexes.[8] In general, for lopsided ligands such as Me_3Bzm, the same number of NMR resonances is expected whether the ligands rotate freely about the Re−N bonds or maintain a fixed orientation. We had established that, in $Re_2O_3Cl_4(Me_3Bzm)_4$ (**3**), aside from the net ∼90° Re−N rotation accompanying inversion of chirality, the Me_3Bzm ligands are unlikely to rotate freely even at ambient *T*.[4] For C_2-symmetrical ligands, such as 3,5-lut, the number of NMR signals expected depends on the rate of 180° rotation about the Re−N bonds. For fast 180° rotation, 3,5-lut would give one sharp resonance for each proton type (i.e., α-H, *β*-H, and *γ*-H), since rotation averages the signals of the chemically but not magnetically equivalent α-H atoms and *β*-H atoms. For very slow 180° rotation, 3,5-lut would give one *γ*-H, but two α-H and two *β*-H signals. Therefore, if at low *T* only Re−N rotation is slowed, broadening is expected for the α-H and *β*-H resonances but not for the *γ*-H signal, since this proton lies on the axis of rotation. However, if Re−O−Re rotation is also slowed, broadening of the *γ*-H signal will also occur. We had established that in **5** the two dynamic processes, i.e., dynamic inversion of chirality and 180° rotation about the Re−N bonds, occur together, on about the same time scale, even though rotation about the Re−O−Re system and the coupled ∼90° rotation is faster than 180° rotation about the Re−N bonds.[4]

Now we apply the above reasoning to the cases of **1** and **2**. First, the number of resonances at 20 °C indicates that at ambient *T* exchange of terminal and stacking positions is fast and that the py and 3,5-lut ligands are in rapid rotation about the Re−N bond on the NMR time scale. At lower *T*, for both *rac* and *meso* dimers the *γ*-H signals broaden (see below for assignments) and then split, indicating that rotation about the Re−O−Re bond system has reached the slow limit. Each *racemic* dimer, **1*rac*** and **2*rac***, has two rotamers in about the same ratio. The low-*T* spectra suggest that the major rotamers (**R1**) are similar, as are the minor rotamers (**R2**). The *meso* dimer appears to have only one rotamer. However, if we assume that all these rotamers maintain the conformation of the $Re_2O_3Cl_4$ unit found in the solid, all rotamers are chiral and exist as enantiomeric pairs. The variable-temperature (VT) NMR spectra of **1*meso*** and **2*meso*** suggest that at low *T* the two halves of the rotamer occupy inequivalent positions; the two halves exchange positions slowly on the NMR time scale.

Moreover, in all cases the low-*T* spectra demonstrate that each α-H and *β*-H resonance of the C_2-symmetric ligands splits into two, thus indicating that rotation about the Re−N(py or 3,5-lut) bond has also decreased to the slow domain on the NMR time scale. In particular, each α-H and *β*-CH_3 resonance of 3,5-lut in the major set splits into two below −60 °C in **2*rac***; the analogous splitting occurred at lower *T* (below −80 °C) in **1*rac***. Since the splitting of the α-H resonances in **1*rac*** is slightly larger than that in the 3,5-lut dimer **2*rac*** (1.55 *vs* 1.30 ppm), this *T* dependence clearly shows that the rate of rotation about the Re−N bond is faster for the py ligands in **1*rac*** than that for the 3,5-lut ligands in **2*rac***.

2D NMR Spectral Results. 2D NMR spectral assignments were performed only on the two isomers of $Re_2O_3Cl_4(3,5\text{-lut})_2(Me_3Bzm)_2$, **2*rac*** and **2*meso***. These isomers have greater solubility and reach the slow-exchange limit at higher *T* than do the corresponding isomers of $Re_2O_3Cl_4(py)_2(Me_3Bzm)_2$. The spectra at ambient *T* demonstrated that the 3,5-lut and py analogs have the same overall structure.

rac*-$Re_2O_3Cl_4(3,5\text{-lut})_2(Me_3Bzm)_2$ (2*rac*).** There are essentially three different types of cross-peaks in the low-*T* NOESY/EXSY spectrum of **2*rac: (i) intraligand NOE peaks; (ii) intraligand exchange peaks (and exchange-NOE peaks); (iii) exchange peaks between **R1** and **R2**. At both −90 and −100 °C there are clear NOE cross-peaks linking adjacent groups of the same ligand in the major conformer **R1**. The signals for 3,5-lut were easily distinguished from those for Me_3Bzm (Figure 4). The assignments of all Me_3Bzm signals were made from

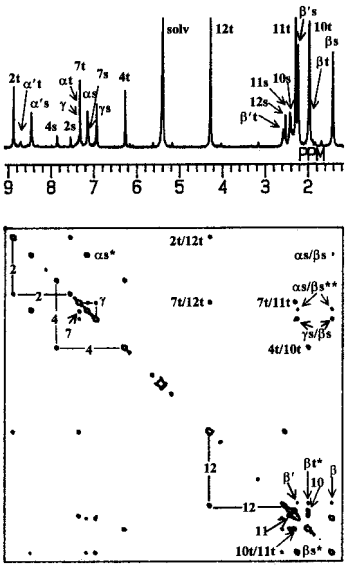

Figure 6. 2D ^{1}H NOESY/EXSY spectrum of ***2rac*** in CD_2Cl_2 at −90 °C. The exchange pathways between **R1** and **R2** are shown. Intramolecular NOE cross-peaks are labeled with the pair of protons involved. Intramolecular exchange cross-peaks are marked with an asterisk. Of the two cross-peaks between αs and βs/β's, marked with two asterisks, one is an NOE cross-peak, while the other is an exchange-NOE cross-peak.

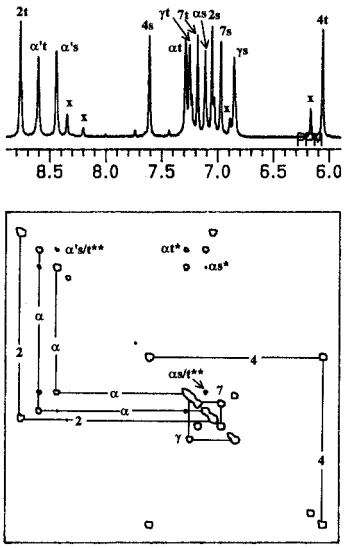

Figure 7. Downfield region of the 2D ^{1}H NOESY/EXSY spectrum of ***2meso*** in CD_2Cl_2 at −100 °C. The exchange pathways between the two halves of the dimer due to the Re−O−Re/Re−N motion are shown. Intramolecular exchange cross-peaks are marked with an asterisk. Exchange cross-peaks due to the combination of 180° Re−N(L) and Re−O−Re/Re−N rotations are marked with two asterisks. A number of minor peaks, due to partial decomposition of ***2meso***, are labeled with x.

the characteristic most downfield B2H signal and the NOE connectivity pathway, 2−12−7−11−10−4 (Chart 1). At −90 °C the pairs of α-H and β-CH_3 resonances of 3,5-lut in **R1** are linked by strong exchange cross-peaks; exchange-NOE cross-peaks between α-H and β-CH_3 resonances are also present due to 180° Re−N rotation that exchanges the two halves of the ligand. Thus, all resonances in **R1** were assigned unambiguously. Moreover, in the NOESY/EXSY spectrum at −90 °C, each resonance of the major set (**R1**), with the exception of α-H (α-H^t resonances are too broad), is related by an exchange cross-peak to a resonance of the minor set (**R2**) (Figure 6), allowing us to assign all resonances of **R2** (Supporting Information). Our assignment of cross-peaks as NOE or exchange peaks was readily confirmed by the NOESY/EXSY spectrum at −100 °C. The intensities of EXSY peaks between **R1** and **R2** decreased considerably; thus, the cross-peak distinction is unambiguous. The sharper 3,5-lut resonances at −100 °C allowed observation of intraligand exchange cross-peaks even for the minor conformer **R2**. Indeed, we could even assign one 3,5-lut α-H resonance of **R2** that overlaps with BH7 of **R1** and γ-H of **R2**.

meso*-$Re_2O_3Cl_4$(3,5-lut)$_2$(Me_3Bzm)$_2$ (2*meso*).** As found for **2*rac, the 3,5-lut signals were easily distinguished from those of Me_3Bzm in the VT spectra of ***2meso*** (Figure 5). In the NOESY/EXSY spectrum at −100 °C the characteristic intraligand NOE connectivity path of the Me_3Bzm signals, besides allowing unambiguous assignment of all Me_3Bzm resonances, allowed designation of the signals belonging to each set. Each Me_3Bzm peak of one set relates to the corresponding peak of the other set via a strong EXSY cross-peak (Figure 7). The direct NOE interactions followed by physical exchange of the ligands produced rather strong exchange-NOE cross-peaks; however, these did not interfere with the assignment.

The division of the 3,5-lut resonances into the two sets was more difficult since all four α-H resonances were interrelated by exchange cross-peaks (Figure 7). Exchange is caused by two contemporaneous dynamic processes: the exchange between the two sets is caused by rotation about the Re−O−Re bonds, and the exchange of α-H with α′−H within each set by 180° rotation of each 3,5-lut about the Re−N bond. A similar exchange pattern was found for the β-CH_3 resonances. The slightly different rotation rate of the 3,5-lut in the two sets allowed us to distinguish unambiguously the α-H resonances belonging to each 3,5-lut. The intraligand NOE pathway, even though affected by the exchange-NOE cross-peaks of comparable intensity, then allowed us to assign the β-CH_3 and γ-H resonances. Interestingly, the exchange cross-peaks between the two sets are more intense than those deriving from the rotation about the Re−N(3,5-lut) bond (in particular for the "slow" set), thus suggesting that, even though both dynamic processes are slow on the NMR time scale, rotation about the Re−N(3,5-lut) bond is the slower. A similar conclusion was reached for $Re_2O_3Cl_4$(3,5-lut)$_4$ (**5**).[4]

The final task of determining which sets of signals belong to which half of the rotamer rested on chemical shift dispersion and the few interligand NOE cross-peaks (see below).

Solution-State Structures. *rac*-$Re_2O_3Cl_4$(3,5-lut)$_2$(Me_3Bzm)$_2$ (2*rac*). In the major rotamer of **2*rac***, **R1**, the shifts of Me_3Bzm are very similar to those of Me_3Bzm^t in $Re_2O_3Cl_4(Me_3Bzm)_4$ (**3**), while the shifts of 3,5-lut are quite similar to those of 3,5-lut^s in $Re_2O_3Cl_4$(3,5-lut)$_4$ (**5**) (Supporting Information).[4] This result demonstrates that the solution conformation of **R1** of **2*rac*** is the same as that found in the solid state of **1*rac***, namely, with 3,5-lut^s and Me_3Bzm^t. The Me_3Bzm ligand can have two orientations differing by 180°, giving a total of three possible conformers. However, it is very likely that the Me_3Bzm^t ligands are oriented as in the solid state of **1*rac***, with the heads pointing toward the negatively charged chloride *trans* to the 3,5-lut^s ligands on the opposite Re atom and each 3,5-lut^s lying on a plane bisecting the *cis* bonds (Figure 1). In agreement with these relative orientations of the Me_3Bzm^t ligands, a deeper cut of the −100 °C NOESY spectrum showed clear NOE cross-peaks between the B4H of Me_3Bzm^t signal and the α-H signals of 3,5-lut^s. Moreover, this structure readily accounts for the shift pattern and, in particular, explains why all signals of 3,5-lut^s are more upfield than the corresponding resonances in **5**. For

Chart 2. The Two Possible HT Conformers of **R2** of the Complex *meso*-$Re_2O_3Cl_4(lut)_2(Me_3Bzm)_2$ (**2*meso***)[a]

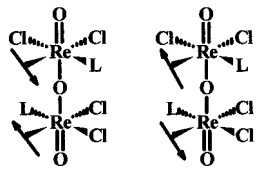

[a] L = 3,5-lut; the arrows represent the Me_3Bzm ligands, with the head being BH2. The eclipsed forms of the dimers are shown.

R1 of **2*rac***, the half of each 3,5-lut^s that is stacked with the other 3,5-lut^s (and whose signals are most upfield) stacks also with the six-membered ring of the adjacent Me_3Bzm^t; Me_3Bzm^t has a greater shielding effect than does the corresponding 3,5-lut^t in **5**. For **R1** of **2*rac***, the other half of each 3,5-lut^s is shielded by the Me_3Bzm^t on the opposite Re atom; again, Me_3Bzm^t has a higher shielding effect than that of the corresponding 3,5-lut^t in **5**.

In **R2** of **2*rac***, Me_3Bzm has shifts similar to those of Me_3Bzm^s in **3**, while 3,5-lut has shifts similar to those of 3,5-lut^t in **5**.[4] The orientation of Me_3Bzm^s in **R2** is very likely the same as in **3**, namely, HT. There are indeed two possible conformers (HT1 and HT2) of **R2** with the Me_3Bzm^s ligands arranged in a HT orientation (Chart 2). In HT1 the arrangement is similar to that found in the crystal structure of **3**; in HT2 both Me_3Bzm^s ligands are rotated by 180°. The following electrostatic and chemical shift arguments strongly indicate that HT1 is by far the most likely. In HT1 the heads of each of the two Me_3Bzm^s ligand points toward the Cl *trans* to 3,5-lut on the opposite Re atom, while in HT2 the heads are pointed to the periphery of the dimer. Thus, only HT1 allows favorable electrostatic interactions. The shifts of Me_3Bzm^s suggest that in solution the HT conformation in **R2** is the same as the HT1 conformation found both in solution and in the solid state for **3**; the B2H, B7H, and $B12H_3$ resonances of the Me_3Bzm^s ligands in **R2** are more downfield than the corresponding resonances in **3** because the shielding effect of the adjacent 3,5-lut^t is lower compared to that of the more anisotropic Me_3Bzm^t in **3**. In the hypothetical HT2 conformer, the five-membered ring of one Me_3Bzm^s would fully stack with the six-membered ring of the other Me_3Bzm^s, and quite different shifts would be expected.

meso*-$Re_2O_3Cl_4(3,5\text{-lut})_2(Me_3Bzm)_2$ (2*meso*).** The two sets of Me_3Bzm NMR signals of **2*meso in the −100 °C NMR spectrum (Supporting Information) can be clearly attributed to Me_3Bzm^t and Me_3Bzm^s from the typical shifts for these ligand types (*cf.* **2*rac*** and **3**). The two sets of 3,5-lut signals can be similarly classified as 3,5-lut^t and 3,5-lut^s signals by comparison with the spectrum of **5**. A more detailed analysis of the shifts and of the solid-state structure provides further insight into the solution conformation of **2*meso***, particularly regarding orientations. These considerations, together with the knowledge acquired with the similar dimers, suggest that the low-*T* conformation of the **2*meso*** dimer closely resembles that found in the solid state.

In the solid state, the head of Me_3Bzm^s is pointing toward the negatively charged chloride *trans* to Me_3Bzm^t on the other Re atom (Figure 2), and only half of 3,5-lut^s is stacked with the Me_3Bzm^s (Figure 3). These features explain the upfield α-H and β-CH_3 resonances for half of 3,5-lut^s. The structure also shows that Me_3Bzm^s is too big to fully stack with 3,5-lut^s. Thus, the methyl on the five-membered ring projects out and is not shielded by 3,5-lut^s, explaining the somewhat more downfield $B12H_3$ signal compared to $B12H_3$ shifts for mutually HT stacked Me_3Bzm ligands, such as in **3** and in **R2** of **2*rac***. In agreement with these relative orientations of the stacked ligands, a deeper cut of the −100 °C NOESY spectrum showed clear NOE cross-peaks between the $B12H_3$ of Me_3Bzm^s signal and the downfield α′-H and β'-CH_3 signals of 3,5-lut^s.

We hypothesize that the orientation of Me_3Bzm^t in **2*meso*** is also close to that found in the solid state, with BH2 pointing toward the chloride *trans* to Me_3Bzm^s on the other Re atom. With this orientation of Me_3Bzm^t, part of its six-membered ring is oriented toward the stacked 3,5-lut on the same Re atom; accordingly, the B4H and $B10H_3$ signals of Me_3Bzm^t are upfield. Moreover, β-CH_3 of 3,5-lut^s is fully stacked with the six-membered ring of Me_3Bzm^s but is also partially stacked with the six-membered ring of Me_3Bzm^t, and this explains why the β-CH_3 resonance falls so far upfield at 0.41 ppm. Also the shifts of 3,5-lut^t suggest that its orientation in solution is very close to that found in the solid state. With this orientation, half of 3,5-lut^t is partially stacked with the five-membered ring of the Me_3Bzm^s on the same Re atom; however, only α-H is fully shielded, and the corresponding signal is shifted upfield, while the adjacent β-CH_3 is only partially shielded, and in fact the corresponding resonance is affected little.

Re−N(L) 180° Rotation. We address first the motions of the symmetrical ligands. EXSY/NOESY spectra established that 180° rotation about the Re−N(3,5-lut) bond occurs in both *racemic* and *meso* dimers. In **2*rac*** (both in **R1** and in **R2**) this motion is faster than the rotation about the Re−O−Re bond system that exchanges stacked and terminal ligands, while the opposite is true in **2*meso***. At −100 °C the exchange process between **R1** and **R2** of **2*rac*** is very slow, and since the splittings of the α-H resonances of 3,5-lut in **R1** and **R2** are comparable, their line widths depend only on the rate of Re−N(3,5-lut) rotation; therefore, the slightly broader α-H signals in **R2** compared to **R1** imply a faster rotation rate of 3,5-lut about the Re−N bond in the minor rotamer; i.e., 3,5-lut^t ligands rotate faster than 3,5-lut^s ligands. In **2*meso*** the splittings of the α-H resonances are very similar in the two sets, but at all temperatures the signals of one set are slightly sharper than those of the other (Figure 4), suggesting that in half of the dimer rotation about the Re−N(3,5-lut) bond is faster than in the other half. In further support of the interpretation of the assignment and structural implications of the *meso* NMR data (see above), 3,5-lut^s rotates about the Re−N bond at a slower rate compared to 3,5-lut^t, which resides in a less sterically demanding region of the dimer.

The case of Me_3Bzm is less straightforward. In all cases the number of Me_3Bzm signals, both in the 20 °C NMR spectra and in each set of the low-*T* spectra, indicates that the Me_3Bzm ligands could either rotate freely about the Re−N bonds or maintain a fixed orientation. In the *meso* dimers the essentially equal broadening of Me_3Bzm signals at all temperatures and the similarity, for each Me_3Bzm resonance, between the average shifts at low *T* and the corresponding shift at high *T* indicate that the Me_3Bzm ligands, as in **3**, are unable to rotate freely at all temperatures. The same conclusion appears to be true also for the *racemic* dimers, but the different abundance of the two rotamers **R1** and **R2** makes comparison of broadening and of shifts at low and high *T* more difficult.

More revealing, analysis of the shifts of the stacked bases in the *meso* isomer indicates that the Me_3Bzm^s does not rotate freely. If it did, there would not be such a large difference in the shifts of the α-H and β-CH_3 signals and the α′-H and β'-CH_3 signals of 3,5-lut. Furthermore, we noted above that there

were several NOE cross-peaks from Me_3Bzm^s to 3,5-lut^s. A bulkier ligand such as Me_3Bzm^s is expected to rotate even more slowly than the smaller 3,5-lut^s ligand, which rotates slowly. Combined, these observations provide compelling evidence that Me_3Bzm^s does not rotate freely.

Similarly, in **R1** of **2*rac*** the NOE cross-peaks between Me_3Bzm^t and 3,5-lut^s indicate that Me_3Bzm does not rotate freely.

Preferred Rotation Pathways for Coupled Re−O−Re/Re−N Rotation. Having established the orientations of the L ligands in **2*rac*** and **2*meso*** and having elucidated the relatively slow rotation, we now consider the coupled dynamic motions. The processes exchange terminal and stacking ligands in a pairwise fashion by a ∼130° rotation about the Re−O−Re bond system (180° minus twice the N^s−Re···Re′−N^s torsion angle) accompanyed by a coupled ∼90° rotation of all four L ligands about the Re−N bonds. In the case of symmetrical dimers **3** and **5**, this process interconverts one enantiomer into the other, since the stable conformation is chiral. For the *racemic* dimers, however, this process does not interconvert one enantiomer into the other, as was the case in symmetrical dimers **3** and **5**, but instead interconverts two rotamers, **R1** and **R2**, each of which is chiral. In a *meso* dimer, the interconversion of the two halves of the dimer is a topomerization between degenerate rotamers to yield the same overall conformation. As for the symmetrical dimers **3** and **5**, this process interconverts one enantiomer into the other, since the stable conformation is chiral. Unstable eclipsed forms of the symmetric and *meso* dimers are not chiral (two halves related by a mirror plane in the *syn* conformation or inversion center in the *anti* conformation). The inversion process must pass through at least one of these unstable eclipsed forms; the form would be either an intermediate or, more likely, an activated complex along the reaction pathway.

We can now evaluate whether the dimers have a preferred pathway of ∼130° rotation about the Re−O−Re bond system, such that the steric repulsions between ligands are minimized and the favorable electrostatic interactions are maximized. In fact, even in the symmetrical dimers **3** and **5** both senses (clockwise or anticlockwise) of Re−O−Re bond system rotation are not equivalent and have different energetic profiles. This is also true in dimers **1** and **2**. In all cases, the pathways would involve an eclipsed form, either *syn* or *anti*. The solution- and solid-state structures of **2*rac***, **2*meso***, and **3** have shown that the positively charged BH2 proton of the Me_3Bzm ligands on one Re atom is always aimed toward the negatively charged chloride on the other Re atom, suggesting that this electrostatic interaction is important and likely to be maintained, if feasible, during rotation. We had found that in *cis*,*cis*,*cis*-$RuCl_2(Me_2SO)_2$(L)(L′) complexes a similar electrostatic interaction strongly influences the solution- and solid-state orientations of the Me_3Bzm ligands.[8]

Coupled Re−O−Re/Re−N Rotation for 2*meso*. The **2*meso*** case will be discussed first. Models show that, starting from the conformation found in the solid state (Figure 2 and top left drawing in Figure 8), anticlockwise rotation of ∼130° of the back Re atom allows the BH2 proton of each Me_3Bzm to remain directed at the chloride *trans* to Me_3Bzm on the other Re atom during the whole process, provided that the contemporaneous 90° rotation of each Me_3Bzm occurs through the O═Re−O coordination plane (CP). The same final Me_3Bzm orientations might be reached through a 270° rotation about each Re−N bond in the opposite sense; this route, besides breaking the favorable electrostatic interactions, would be greatly disfavored by steric interactions.

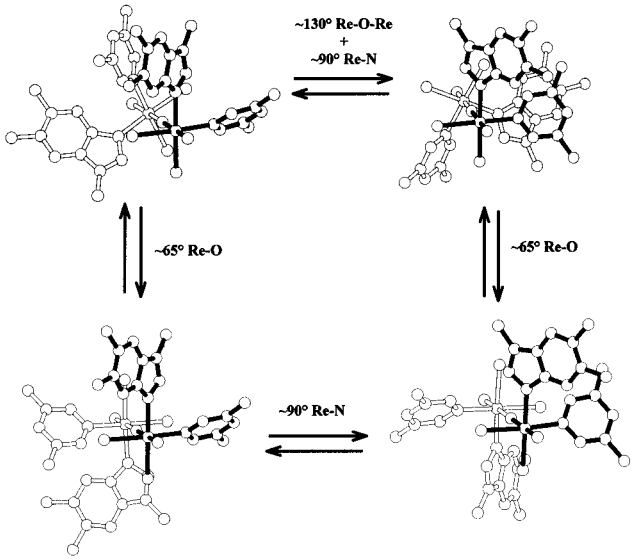

Figure 8. Schematic representation of the dynamic motion proposed for the exchange in solution of the two halves of the dimer in **2*meso***, through the unstable *anti* form. The initial conformation (top left) was found in the solid. Ligands on the front Re atom have shaded bonds.

The 3,5-lut ligands must also undergo 90° Re−N rotation coupled with the Re−O−Re rotation. There are two possible rotation pathways, either through the O═Re−O CP or in the opposite sense through the Cl2−Re−N(Me_3Bzm) CP. Models show that while 90° rotation through the O═Re−O CP physically exchanges the stacked half of 3,5-lut^s with the unstacked half of 3,5-lut^t (i.e., in terms of resonances α′s with αt and αs with α′t), the 90° rotation through the Cl2−Re−N(Me_3Bzm) CP exchanges the stacked half of 3,5-lut^s with the stacked half of 3,5-lut^t (i.e., in terms of resonances α′s with α′t and αs with αt). At −100 °C 180° Re−N(3,5-lut) rotation is slow compared to the coupled Re−O−Re/Re−N rotation, and therefore the most intense exchange cross-peaks are those relating protons directly exchanged by the coupled motion. Thus, a close examination of the intensity of the exchange cross-peaks in the −100 °C EXSY spectrum should allow us to distinguish between the two possible 90° rotation pathways. In agreement with the O═Re−O CP pathway, the most intense exchange cross-peaks in the downfield region of the EXSY spectrum (Figure 7) are those relating α′s with αt and αs with α′t (similar conclusions are drawn from the upfield β resonances). This preferred sense of rotation for both 3,5-lut ligands in **2*meso*** is the same as we established for $Re_2O_3Cl_4(3,5\text{-lut})_4$,[4] in which the 3,5-lut ligands also rotate through the less sterically demanding O═Re−O CP. Thus, a consistent picture emerges.

It is very likely that the two coupled movements in the favored route, ∼130° Re−O−Re rotation and ∼90° Re−N rotation, occur sychronously, but for the sake of discussion, as done previously for **5**, the process can be broken into three distinct steps (Figure 8).[4] In the first step, a ∼65° Re−O rotation forms an unstable *anti* species; in the next step, the two Me_3Bzm ligands and the two 3,5-lut ligands rotate by 90° past the respective O═Re−O CPs. Finally, a second ∼65° Re−O−Re rotation in the same direction as the first converts the unstable *anti* species to the other topomer, which is the enantiomer of the starting conformer.

Rotation about the Re−O−Re bond system in the opposite sense would not only interrupt the favorable electrostatic interactions for both Me_3Bzm ligands, but also bring the N-donor ligands much closer to each other, through an unstable *syn eclipsed* form. Therefore, this pathway is unlikely.

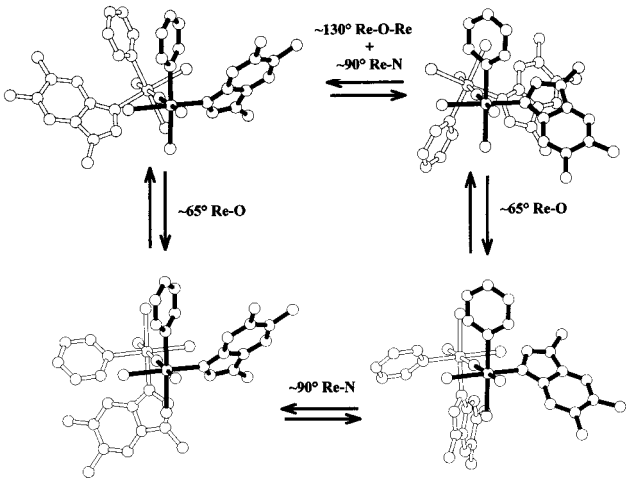

Figure 9. Schematic representation of the dynamic motion proposed for the exchange in solution between **R1** and **R2** in **1*rac***, through the unstable *anti* form. The initial conformation (top left) was found in the solid. Ligands on the front Re atom have shaded bonds.

Coupled Re−O−Re/Re−N Rotation for 2*rac*. As already pointed out, in the racemic dimer **2*rac***, the ∼130° Re−O−Re rotation interconverts two rotamers, **R1** and **R2**, each of which is chiral. Unlike the cases of **2*meso***, **3**, and **5**, 90° Re−N rotation of the four L ligands is not required by symmetry to be coupled to the Re−O−Re rotation. Chemical shift arguments for Me_3-Bzm ligands led us to believe that this 90° Re−N rotation indeed occurs for the two lopsided ligands. Models show that, starting from the solid-state conformation of **1*rac*** (**R1**, Figure 1 and top left structure in Figure 9), ∼130° anticlockwise rotation about the back Re−O bond that converts Me_3Bzm^t ligands into Me_3Bzm^s ligands must be accompanied by a 90° rotation of both Me_3Bzm ligands about the Re−N bond to achieve one of the two HT conformations. A 90° rotation in one direction, i.e., across the O═Re−O CP, will give the favored HT1 conformer.[17] During the process transforming **R1** into **R2**, the BH2 proton in each of the two Me_3Bzm ligands remains aimed at the chloride *trans* to 3,5-lut on the other Re atom and by passage through an *anti* form avoids steric clashes between ligands. Conversely, 90° Re−N(Me_3Bzm) rotation in the opposite direction, i.e., through the Cl−Re−N(3,5-lut) CP, would be disfavored both sterically and electrostatically and would, in any case, yield the HT2 conformer, which the NMR evidence indicates is not present.

As depicted schematically in Figure 9, models show that 90° rotation very likely occurs for the 3,5-lut ligands also. This reasoning is also based on both steric and shift considerations. If such 90° rotation did not occur, in **R2** one α-H on each 3,5-lut would be too close to the BH2 of the *cis* Me_3Bzm ligand; moreover, the 3,5-lut^t would not be partially stacked with the five-membered ring of the *cis*-Me_3Bzm^s, and more downfield shifts might be expected for 3,5-lut^t ligands.

Finally, as for **2*meso***, for **2*rac*** the opposite-sense ∼130° Re−O−Re rotation is disfavored for electrostatic and steric reasons since it involves the *syn* eclipsed form. In summary, it is likely that both in the *meso* and in the *racemic* dimers, the two halves of the dimer swing back and forth by ∼130° through the *anti* eclipsed species.

Conclusions

Previously we investigated the dynamic exchange between degenerate chiral conformers. The synthesis of mixed-ligand μ-oxorhenium dimers that bear one lopsided and one symmetrical ligand, $Re_2O_3Cl_4(py)_2(Me_3Bzm)_2$ (**1**) and $Re_2O_3Cl_4(3,5\text{-}lut)_2(Me_3Bzm)_2$ (**2**), has now allowed us to break the local symmetry on each rhenium atom, so that, in the racemic dimers, the exchange of terminal and stacked ligands leads to nondegenerate conformers. We found that the solution conformation of **R1** is the same as that found in the solid state of **1*rac***. Moreover, in the case of both **1*rac*** and **2*rac***, the conformer with terminal Me_3Bzm ligands (**R1**) is roughly 1 order of magnitude more stable than that with stacking Me_3Bzm ligands (**R2**). We believe that the stability of **R1** over **R2** can be attributed mainly to more favorable electrostatic interactions that occur between the δ^+ H2 atoms on Me_3Bzm^t ligands and the negative O and Cl groups in the core of the dimer.[18] This interaction, which is evident from the orientation of the Me_3-Bzm in the structures of all three dimers having Me_3Bzm, appears to overcome the stacking interactions in the **R2** conformer of **1*rac*** and **2*rac***.

NMR data showed that the unsymmetrical dimers **1** and **2** undergo two dynamic processes contemporaneously, namely, 180° rotation about the Re−N(py or 3,5-lut) bond and coupled rotation about the Re−O−Re/Re−N bonds. Both processes reach the slow-exchange limit for $T < -80$ °C. Rotation of py in **1** occurs faster than that of 3,5-lut in **2**; this difference is attributed to the higher steric demands of 3,5-lut compared to py. NMR data provide compelling evidence that Me_3Bzm ligands do not rotate freely in the *meso* compounds. For the *racemic* compounds, it is likely that each Me_3Bzm rotates only ca. 90° about the N−Re bond and adopts the orientation such that it maximizes the electrostatic attractions in **R1** (Me_3Bzm^t) and minimizes the steric crowding in **R2** (Me_3Bzm^s) during the **R1** to **R2** conversion. Thus, a consistent, rather satisfying view of the dynamic motion pathways for planar N-heterocyclic ligands emerges from our studies of these dimers. The principles established should have wide application in metallobiochemistry.

Acknowledgment. This work was supported by the Italian MURST in the frame of the Project "Pharmacological and Diagnostic Properties of Metal Complexes" (coordinator Professor G. Natile), and by the NIH (Grant GM 29222). We thank the CNR staff at ELETTRA for their help in the use of the facility supported by CNR and by the Elettra Scientific Division.

Supporting Information Available: Two X-ray crystallographic files, in CIF format, and tables with ^{1}H NMR assignments. This material is available free of charge via the Internet at http://pubs.acs.org.

IC990858T

(17) As for **2*meso***, the opposite 270° Re−N(Me_3Bzm) rotation is disfavored for electrostatic and steric reasons.

(18) Marzilli, L. G.; Marzilli, P. A.; Alessio, E. *Pure Appl. Chem.* **1998**, *70*, 961−968.